

# Giant field enhancement by funneling effect into sub-wavelength slit-box resonators

Paul Chevalier,<sup>1,2</sup> Patrick Bouchon,<sup>2,\*</sup> Riad Haïdar,<sup>2,3</sup> and Fabrice Pardo<sup>1</sup>

<sup>1</sup>*Laboratoire de Photonique et de Nanostructures (LPN-CNRS),  
Route de Nozay, 91460 Marcoussis, France*

<sup>2</sup>*ONERA, The French Aerospace Lab, 91761 Palaiseau, France*

<sup>3</sup>*École Polytechnique, Département de Physique, 91128 Palaiseau, France*

(Dated: May 4, 2021)

## Abstract

Inspired by the acoustic Helmholtz resonator, we propose a slit-box electromagnetic nanoantenna able to concentrate the energy of an incident beam into surfaces a thousand times smaller than with a classical lens. This design gives birth to giant field intensity enhancement in hot volume, throughout the slit. It reaches  $10^4$  in the visible up to  $10^8$  in the THz range even with focused beams thanks to an omnidirectional reception. These properties could target applications requiring extreme light concentration, such as SEIRA, non-linear optics and biophotonics.

Optical nanoantennas are of great importance for harvesting light from the free space to deep-subwavelength volume and to reach a strong electric field enhancement [1–8]. They have a wide range of applications including surface enhanced Raman scattering (SERS) [9], photovoltaics and photodetection [10], non-linear optics [11], bio-sensing [12], surface enhancement infrared absorption (SEIRA) [13–15], and thermal emission [16]. Field intensity enhancement up to  $10^3$  was observed using subwavelength particles [17] and an enhancement up to  $10^6$  is expected inside self-similar chains [18]. Inspired by radiofrequency designs, various nanoantennas have been engineered to improve the field enhancement in larger volumes, such as bow-tie [19, 20], quarter-wave or Yagi-Uda [21–23] antennas. However, the antennas previously proposed either concentrate the electric field only in *hot spots*, or are plagued by their directivity which prevents them to be used with focused beam. The key issue to further enhance the electromagnetic field is thus to design an antenna having a large angular acceptance as well as a wide cross-section. Here, we present a slit-box resonator inspired by the acoustic Helmholtz resonator [24], which is able to omnidirectionally funnel all the light through its aperture regardless of its width, leading to million fold electric field intensity enhancement in a *hot volume*. This design, allows to tune independently the slit (width:  $w$ , height:  $h$ ) and the cavity geometries for a given resonance wavelength  $\lambda$  and we demonstrate that it leads to a giant enhancement factor driven by the ratio  $\lambda^2/(hw)$ . This enhancement factor only depends slightly on the angle of incidence which permits to use this antenna at the focal spot of a classical lens to further strongly enhance the electric field intensity. This giant field intensity enhancement opens great perspectives of application for devices based on SEIRA or nonlinear optics which used focused beam.

The funneling by magneto-electric interference was shown to efficiently collect light into 2D sub-wavelength slits with a near- $\lambda$  cross section and a large angular acceptance [25–28]. In the following, the funneling effect is applied to a single Helmholtz-like nanoantenna at the focal point of a focused beam. Our electromagnetic structure is made of a metallic material and is long enough along the  $\mathbf{y}$  direction to be considered as infinite. It consists in a box (width  $w_b$ , height  $h_b$ ) and a slit (width  $w_s$ , height  $h_s$ ) as shown in Fig. 1(a). A beam is focused on one of these structures where almost all the incident energy is funneled. Exact Maxwell computations [29] of this slit-box resonator are performed by considering that the metallic walls are made of gold. Its dielectric function is computed from the Drude model  $\varepsilon_{\text{Au}}(\lambda) = 1 - [(\lambda_p/\lambda + i\gamma) \lambda_p/\lambda]^{-1}$  which matches well the experimental data in the

infrared domain for  $\lambda_p = 159 \text{ nm}$  and  $\gamma = 0.0077$  [30]. In the following we consider a box of width  $w_b = 49 \text{ nm}$  and of height  $h_b = 49 \text{ nm}$ , and a slit of width  $w_s = 2.5 \text{ nm}$  and of height  $h_s = 11 \text{ nm}$  [31] that is firstly studied at  $\lambda = 1.7 \mu\text{m}$ .

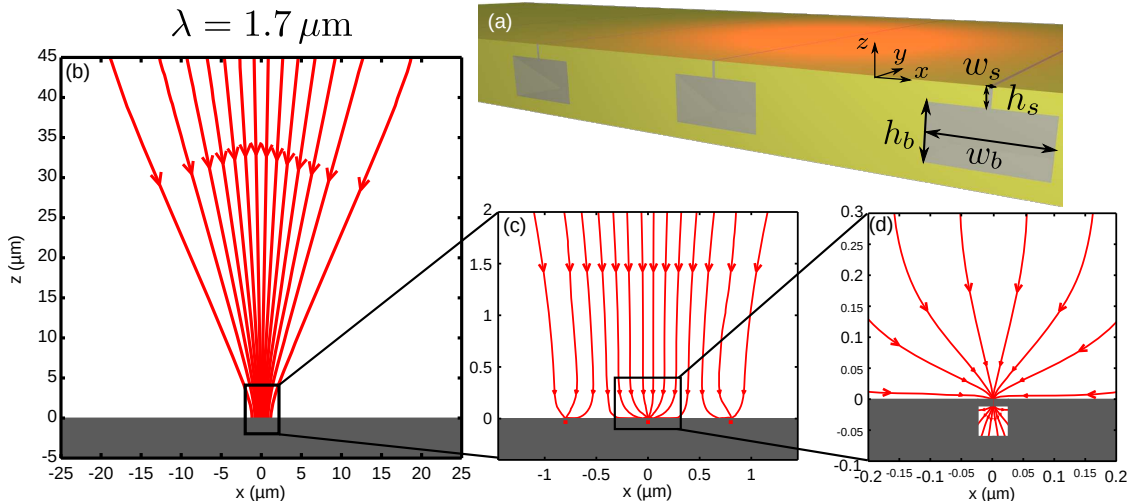


FIG. 1. (a) A beam is focused on a structure made of a slit of width  $w_s = 2.5 \text{ nm}$  and height  $h_s = 11 \text{ nm}$  ended by a box of width  $w_b = 49 \text{ nm}$  and height  $h_b = 49 \text{ nm}$ . (b) Streamlines of the beam focused into the structure, the beam waist is about  $\lambda = 1.7 \mu\text{m}$  wide. (c) The beam is focused on one individual structure that collects about 60 % of the incoming energy. The remaining energy is fully collected by the neighboring slits. (d) Streamlines of the Poynting vector in the vicinity of the structure, showing that the magneto-electric interference redirects the incident energy inside the resonator [25].

The behavior of the structure has been simulated by focusing a beam onto a slit-box structure. Technically the structure is periodized with a period  $d = 0.8 \mu\text{m}$  slightly smaller than the wavelength (see supplementary materials). The streamlines of the Poynting vector plotted at a large scale in Fig. 1(b) show that the incident energy is focused into a beam limited by diffraction (see Fig. 1(c)) where 90% of the energy is concentrated in a  $\lambda$ -wide spot (here the wavelength is  $\lambda = 1.7 \mu\text{m}$ ). Next, in the near field ( $z < 500 \text{ nm}$ , see Fig. 1(d)), all the focused energy is funneled towards the opening of the resonators where it is absorbed on the metallic sidewalls. In fact, given the size of the focal spot, 60% of the total energy is absorbed by the central resonator while the remaining energy is equally absorbed by the two surrounding resonators. Since the incoming energy goes through the slit of the resonator, the electric field intensity is strongly enhanced in the whole slit volume.

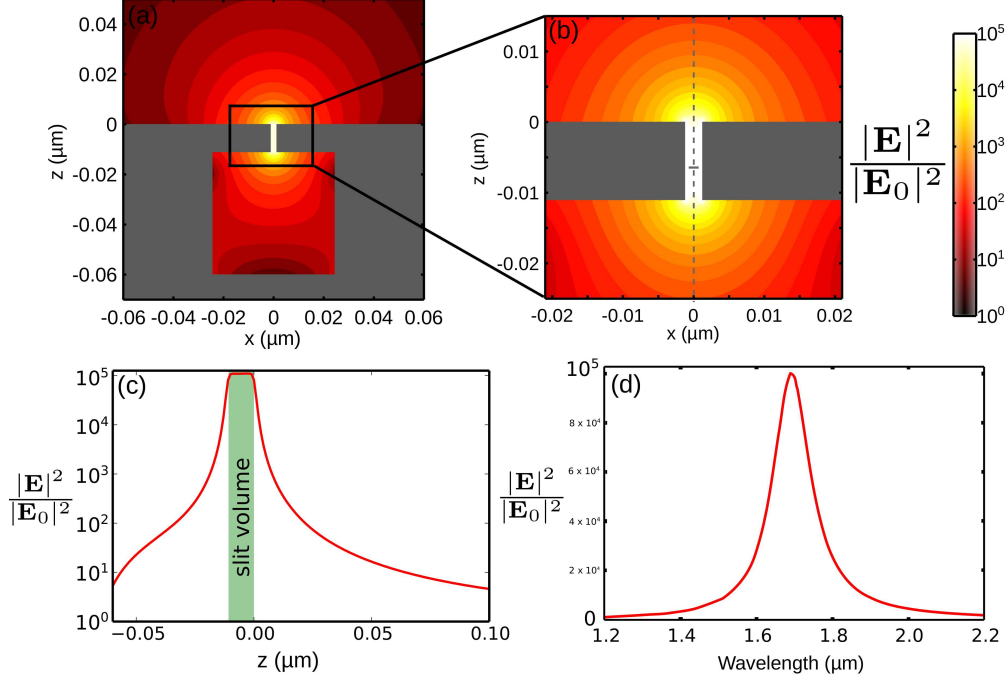


FIG. 2. The electric field intensity enhancement is shown at different scales for an incident focused beam. (a) Global field intensity enhancement at  $\lambda = 1.7 \mu\text{m}$ . (b) Close view in the vicinity of the slit. (c) Field intensity enhancement along the  $z$ -axis, at the center of the structure ( $x = 0$ ). A rather homogeneous enhancement of  $10^5$  is found in the whole slit volume. (d) The field intensity enhancement in the center of the slit is plotted at different wavelengths. We see that  $\lambda = 1.7 \mu\text{m}$  is a resonance wavelength that provide a maximal enhancement. The quality factor of this resonance is about 10.

The distribution of the electric field intensity ( $|E|^2$ ) normalized by the incident field intensity ( $|E_0|^2$ ) in the central structure is presented in Figs. 2(a)-2(b) at different zoom levels and shows that a field intensity enhancement of  $10^5$  is reached with this structure. In Fig. 2(c), it is shown that this enhancement is confined to the slit volume: the field intensity enhancement stays constant along the height of the slit, but outside its volume the electric field intensity quickly drops by losing 4 orders of magnitude over about 50 nm. Noteworthy, this profile of the electric field departs from the behaviour of a Fabry-Perot slit, and it adds to the fact that the slit-box resonator does not exhibit harmonics features (see

Fig. S1 in supplemental materials.) The quality factor is  $Q \simeq 10$  for a resonance wavelength of  $\lambda_R = 1.7 \mu\text{m}$  as shown in Fig. 2(d). In the supplementary materials, we show that the slit-box structure is fairly well described by a LC resonator model (the capacitor being the slit, and the inductance being the box that acts as a magnetic energy accumulator), giving an analytic formula for the resonance wavelength:  $\lambda_R \simeq 2\pi n_s \sqrt{w_b h_b h_s / w_s}$  where  $n_s$  is the refractive index of the dielectric material filling the slit. It must be emphasized that, as expected from the inductive nature of the box, its dielectric filling plays no role on the resonance wavelength.

For an incident wave polarized with the electric field perpendicular to the slits, the maximum field intensity enhancement  $G_{max}$  in the slit at the resonance can be expressed as:

$$G_{max} = \frac{|E_{max}|^2}{|E_0|^2} = \frac{Q}{2\pi} \frac{\lambda^2}{h_s w_s}, \quad (1)$$

where  $Q$  is the quality factor of the resonance,  $\lambda$  is the wavelength. This formula stems from the expression of the stored energy and the dissipated energy inside the resonators (see supplementary materials). It stands for a plane wave normally incident onto a perfectly impedance-matched structure, exhibiting total absorption (i.e. neither scattered nor reflected fields). In a more general situation, where the energy absorption efficiency  $A$  is different from 1, or when the period  $d$  is different from  $\lambda$ , the field intensity enhancement writes  $G = \frac{Q}{2\pi} \frac{A\lambda d}{h_s w_s}$ . In figure 3 the enhancement factor has been calculated for variously shaped structures ( $\varepsilon_s = 1$ ) exhibiting resonances from the near infrared to the far infrared and is plotted as a function of  $G$ . This figure shows the good agreement between this analytic model and the values obtained through numerical simulations in the different domains of frequencies.

The angular dependence of the enhancement is studied in Fig. 4. The general configuration of conical incidence is described in Fig. 4(a), the light is impinging on the antenna with an angle  $\vartheta$  in the plane defined by the azimuthal angle  $\varphi$  and is polarized so that the magnetic field is in the  $y - z$  plane. The enhancement  $G$  as a function of both angles is plotted in Fig. 4(b). It remains above  $5 \cdot 10^4$  for angle of incidence below  $35^\circ$  which demonstrates the omnidirectional behaviour of the resonator. Due to its high angular tolerance, the enhancement  $G$  would only be slightly reduced when the structure is placed at the focal spot of a lens. In this case, the electric field intensity  $|E|^2$  would be similar to the one obtained if, beyond the limits of diffractive optics, a beam of given power was focused in a

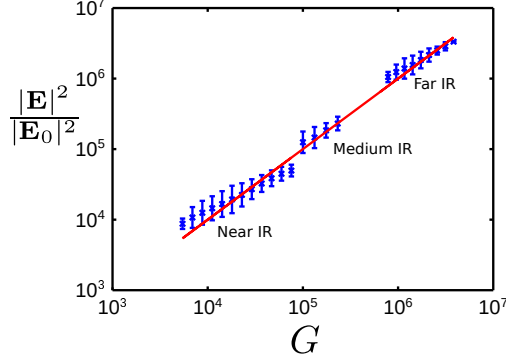


FIG. 3. Simulations for different size of structure have been realized with  $\varepsilon_s = 1$ . For each structure the field intensity enhancement for a plane incident wave is computed and compared to the model provided here. We see a strong correlation between the simulations results and the formula provided in the manuscript for the different domains of frequency. Three sets of simulations have been made, the first in the near IR domain ( $\lambda$  between  $2 \mu\text{m}$  and  $8 \mu\text{m}$ ), the second in the medium IR ( $\lambda$  between  $10 \mu\text{m}$  and  $25 \mu\text{m}$ ) and the last in the far IR domain ( $\lambda$  between  $30 \mu\text{m}$  and  $80 \mu\text{m}$ )

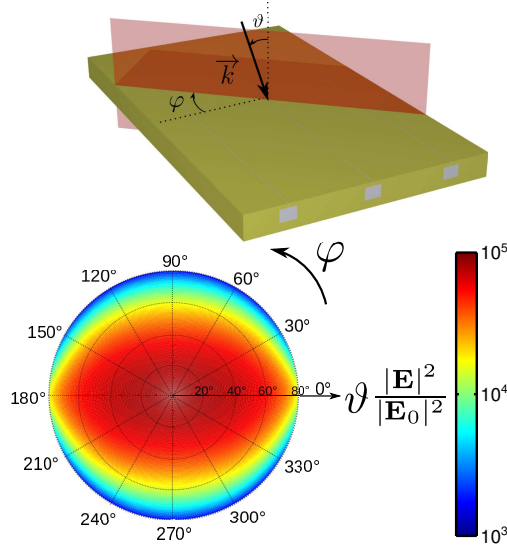


FIG. 4. The electric field intensity enhancement is computed for an incident plane wave (polarized parallel to the slits) with different angles of incidence and different planes of incidence. The structure is the same as described in the manuscript. (a) The plane of incidence is rotated by an angle  $\varphi$ , the angle of incidence is  $\vartheta$ . (b) The results of the field intensity enhancement is represented with polar coordinates on the right. The field intensity enhancement remains above  $5 \times 10^4$  for angles of incidence below  $40^\circ$ , it is above  $10^4$  for angle of incidence below  $65^\circ$ .

spot of area  $\lambda^2/G$  instead of  $\lambda^2$ . Noteworthy, this intensity is uniformly obtained in a “hot volume” of height  $h_s$  and area  $\lambda w_s \gg \lambda^2/G$ .

Very strong field intensity enhancements can be reached not only in the infrared range, but in the whole spectrum from visible to THz domain. At higher wavelengths, losses in the metal are weaker than in the near IR, so the quality factor of the resonance is greater. Therefore, higher field intensity enhancements will be reached at longer wavelengths. As shown in the supplementary materials, such structures allow higher enhancement factors for the intensity of the electric field than in the literature:  $10^5$  vs.  $10^3$  [8, 13, 15, 17] in the near IR or visible,  $10^6$  vs.  $10^4$  in the far IR [32], and  $10^8$  vs.  $10^6$  in the THz domain [33].

The slit-box structure allows to funnel nearly all the incident energy through the arbitrarily narrow aperture of the slit leading to giant enhancement of the electric field in the whole slit volume. These appealing properties are very promising for light matter interactions such as in photodetection, SERS, SEIRA and non-linear optics.

We are thankful to J.-J. Greffet for precious discussions concerning this manuscript. We acknowledge financial support from the ONERA through the SONS project.

---

\* patrick.bouchon@onera.fr

- [1] G. Lerosey, J. de Rosny, A. Tourin, and M. Fink, *Science* **315**, 1120 (2007).
- [2] A. Grbic, L. Jiang, and R. Merlin, *Science* **320**, 511 (2008).
- [3] Z. Zhang, R. Peng, Z. Wang, F. Gao, X. Huang, W. Sun, Q. Wang, and M. Wang, *Applied Physics Letters* **93**, 171110 (2008).
- [4] L. Novotny and N. van Hulst, *Nature Photonics* **5**, 83 (2011).
- [5] P. Biagioni, J.-S. Huang, and B. Hecht, *Reports on Progress in Physics* **75**, 024402 (2012).
- [6] W. Barnes, A. Dereux, T. Ebbesen, *et al.*, *Nature* **424**, 824 (2003).
- [7] J.-J. Greffet, *Science* **308**, 1561 (2005).
- [8] J. Schuller, E. Barnard, W. Cai, Y. Jun, J. White, and M. Brongersma, *Nature Materials* **9**, 193 (2010).
- [9] T. Siegfried, Y. Ekinici, O. J. F. Martin, and H. Sigg, *Nano Letters* **13**, 5449 (2013), <http://pubs.acs.org/doi/pdf/10.1021/nl403030g>.
- [10] M. Knight, H. Sobhani, P. Nordlander, and N. Halas, *Science* **332**, 702 (2011).

- [11] M. Kauranen and A. V. Zayats, *Nature Photonics* **6**, 737 (2012).
- [12] N. Liu, M. L. Tang, M. Hentschel, H. Giessen, and A. P. Alivisatos, *Nature materials* **10**, 631 (2011).
- [13] D. Dregely, F. Neubrech, H. Duan, R. Vogelgesang, and H. Giessen, *Nature communications* **4** (2013).
- [14] J. Bochterle, F. Neubrech, T. Nagao, and A. Pucci, *ACS nano* **6**, 10917 (2012).
- [15] R. Adato, A. A. Yanik, J. J. Amsden, D. L. Kaplan, F. G. Omenetto, M. K. Hong, S. Erramilli, and H. Altug, *Proceedings of the National Academy of Sciences* **106**, 19227 (2009).
- [16] J. A. Schuller, T. Taubner, and M. L. Brongersma, *Nature Photonics* **3**, 658 (2009).
- [17] P. Mühlischlegel, H. Eisler, O. Martin, B. Hecht, and D. Pohl, *Science* **308**, 1607 (2005).
- [18] K. Li, M. I. Stockman, and D. J. Bergman, *Physical Review Letters* **91**, 227402 (2003).
- [19] P.J. Schuck, D.P. Fromm, A. Sundaramurthy, G.S. Kino, and W.E. Moerner, *Physical Review Letters* **94**, 017402 (2005).
- [20] S. Kim, J. Jin, Y.-J. Kim, I.-Y. Park, Y. Kim, and S.-W. Kim, *Nature* **453**, 757 (2008).
- [21] L. Novotny, *Phys. Rev. Lett.* **98**, 266802 (2007).
- [22] T. Kosako, Y. Kadoya, and H. F. Hofmann, *Nature Photonics* **4**, 312 (2010).
- [23] D. Dregely, R. Taubert, J. Dorfmueller, R. Vogelgesang, K. Kern, and H. Giessen, *Nature communications* **2**, 267 (2011).
- [24] H. von Helmholtz, *Theorie der Luftschwingungen in Röhren mit offenen Enden*, 80 (W. Engelmann, 1896).
- [25] F. Pardo, P. Bouchon, R. Haidar, and J.L. Pelouard, *Physical Review Letters* **107**, 093902 (2011).
- [26] P. Bouchon, F. Pardo, B. Portier, L. Ferlazzo, P. Ghenuche, G. Dagher, C. Dupuis, N. Bardou, R. Haïdar, and J. Pelouard, *Applied Physics Letters* **98**, 191109 (2011).
- [27] G. Subramania, S. Foteinopoulou, and I. Brener, *Phys. Rev. Lett.* **107**, 163902 (2011).
- [28] P. Chevalier, P. Bouchon, R. Haïdar, and F. Pardo, *Journal of Nanophotonics* **6**, 063534 (2012).
- [29] P. Bouchon, F. Pardo, R. Haïdar, and J. Pelouard, *Journal of the Optical Society of America A* **27**, 696 (2010).
- [30] E. Palik and G. Ghosh, *Handbook of optical constants of solids* (Academic press, 1985).
- [31] Since we do not take into account the non localities and quantum effects, this model for the

strong field intensity enhancement is valid for slits of widths greater than 2 nm [34].

- [32] C. Feuillet-Palma, Y. Todorov, A. Vasanelli, and C. Sirtori, *Scientific Reports* **3** (2013).
- [33] M. Seo, H. Park, S. Koo, D. Park, J. Kang, O. Suwal, S. Choi, P. Planken, G. Park, N. Park, *et al.*, *Nature Photonics* **3**, 152 (2009).
- [34] R. Esteban, A. G. Borisov, P. Nordlander, and J. Aizpurua, *Nature Communications* **3**, 825 (2012).